ACS FOOD SCIENCE & TECHNOLOGY

pubs.acs.org/acsfoodscitech

Article

Naked-Eye Food Freshness Detection: Innovative Polymeric Optode for High-Protein Food Spoilage Monitoring

Lisa Rita Magnaghi,* Giancarla Alberti, Chiara Milanese, Paolo Quadrelli, and Raffaela Biesuz

Cite This: *ACS Food Sci. Technol.* 2021, 1, 165−175

Read Online

ACCESS | Metrics & More | Article Recommendations | Supporting Information

ABSTRACT: An innovative smart label for naked-eye protein food freshness evaluation, based on polymeric sensing films, is presented. The proposed device consists of six miniaturized sensors, obtained by covalently binding six pH indicators, namely, *m*-cresol purple (**1**), *o*-cresol red (**2**), bromothymol blue (**3**), thymol blue (**4**), chlorophenol red (**5**), and bromophenol blue (**6**), to an ethylene vinyl alcohol (EVOH) copolymer. All of the synthetic procedures for the functionalized polymers and their application as smart labels are thoroughly described and discussed. The innovative sensors are characterized using several instrumental techniques (DSC, FT-IR, EDX, SEM, and UV−vis). The application of the array of sensors to poultry meat and cod fillet spoilage monitoring by naked-eye evaluation and modeling by PCA is presented. Eventually, the composition of the food and the food's headspace in the selling tray is investigated and qualitatively characterized to validate the attributes of the array of sensors. The polymeric devices seem to be very promising for industrial scale-up, with the starting EVOH copolymer being extrudable and already employed in food packaging, as well as for large-scale application, being clear, efficient, and easy to read, even by untrained people.

KEYWORDS: *EVOH functionalization, polymer-based optode, naked-eye smart labels, protein foods, PCA, instrumental validation*

INTRODUCTION

A complex combination of bacterial processes determines food spoilage, and monitoring these events is a pivotal consumer demand in light of maintaining a high qualitative standard of foods in general.[1] Among all foodstuffs, aliments of animal origin, with a particular focus on meat and fish, require special attention. In fact, the decay of quality in meat is fast, because microorganism activities can quickly increase,[2] and can also be affected by several factors during distribution.[3−5] Considering these assumptions, it goes without saying that the traditional, expensive, time-consuming methods commonly employed for meat spoilage monitoring are definitely inadequate and must be updated or even replaced by rapid, low-cost, and nondestructive techniques.[2,6−8]

Because this has been a hot topic in the past several years and involves primary economic and health interests, a wide variety of sensing approaches have been tested for these applications, ranging from biosensors[9,10] and electronic devices[7,11,15] to colorimetric devices.[2,6,12−14,16−21] Among all, the colorimetric devices, especially those relying on pH indicators as the sensing unit, seem to be highly promising for a naked-eye evaluation of food freshness based on two simple pillars. First, the use of colors is extremely convenient for a consumer as well as for the packaging producers without any remarkable additional costs for labeling and packing different foods. Second, the use of several pH indicators, having different log K_a values to cover a wide pH range, ensures a reliable methodology for food degradation evaluation. In fact, for each degradation step, the distinctive volatile byproducts have a different acid−base behavior, resulting in changes in the acidity of the headspace over meat samples during its spoilage.[5,22,23] Nevertheless, some common weak points can be individuated in the papers dealing with this topic.[8] First and foremost, biogenic amines (BAs) have been undeservedly granted a leading role in freshness detection but have never been detected in meat headspace during a storage time typical of a real-life situation.[8,24,25]

In this scenario, there is a growing need for an efficient sensing approach that allows the entire degradation process to be monitored, on the basis of the chemical spoilage index (CSI) and volatile byproducts typical of each degradation step, rather than on the most famous ones.[3−5,22,23] In the early spoilage, CSI is associated with the consumption of glucose and lactic acid and the production of EtOH, 3-methyl-1-butanol, and free fatty acids, mainly acetic acid,[23] which are definitively the dominant VOCs. As a result, their release provokes a slight increase of the acidity in the headspace. At this stage, protein foods are a safe product and thus a proper sensing device must exhibit the ability to recognize this stage.

Only when no more glucose and none of its direct metabolites are left, the catabolism of proteins starts, and the production of amines and thiols is manifested as off-odors and discoloration.[23] Due to the toxicity of these classes of byproducts, consumption of meat at this stage could be a severe hazard, but as suggested above, BAs, actually produced into protein foods, cannot be found in the headspace, where sensing devices are usually included.[8,24,25] This aspect can be explained considering that BAs are weak bases, involved in one or more protonation

Received: November 9, 2020
Revised: December 15, 2020
Accepted: December 22, 2020
Published: December 31, 2020

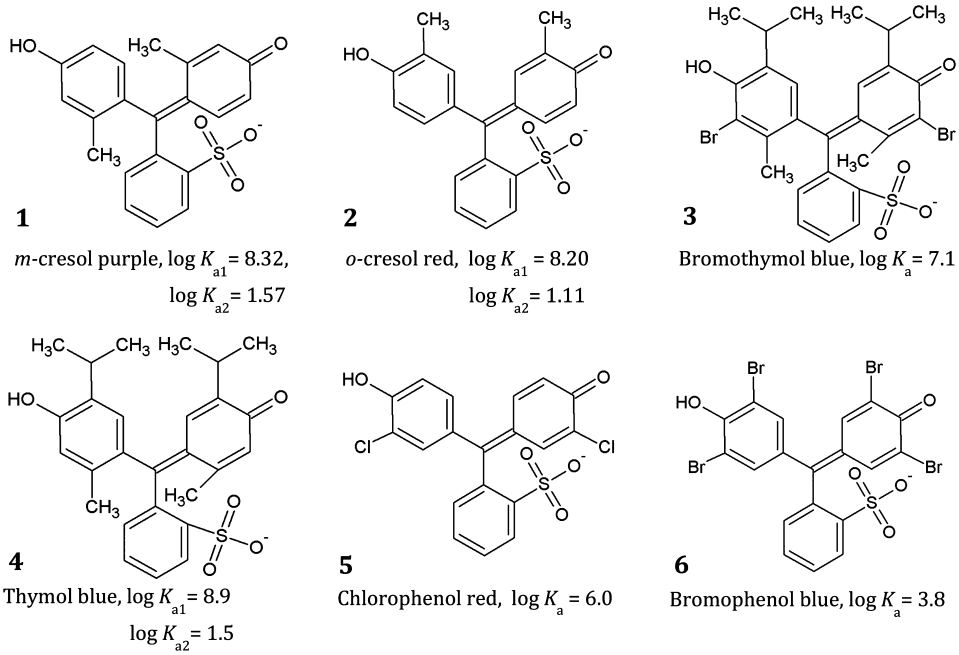

Figure 1. Chemical formulas of the dyes employed as sensing moieties, together with the log K_a values reported in the literature.[28−30]

equilibria between species with a different charge. Because only neutral molecules diffuse through the interface with air, their volatility depends on the pH of the medium. In the case of meat and other biological matrices, the pH is buffered at a value around neutrality at which the amines are present in their positively charged protonated form and thus cannot diffuse into the air. On the basis of this knowledge, an optode that can detect a slight decrease in the acidity of the headspace, always around neutrality, represents the best sensing device for monitoring protein food degradation. Conversely, the selection of pH indicators that turn their color at basic or extremely basic pH as receptors could seem to be a promising strategy when analyzing synthetic samples or enriched ones[13,21] but would fail the test in the case of the degradation of real samples under home conditions.

A very first "proof of concept" based on this approach has been already presented in previous works[8,24,25] in which the receptors were temporarily embedded into an anion exchange cellulose sheet, Color Catcher (CC), via ion exchange, to select the most informative pH indicators and, mainly, to identify the best design strategy for assuring glaring and well-defined color changes to avoid any misunderstanding.

Because the ion exchange mechanism is not compatible with a large-scale application in the food field, due to the risk of dye release when in contact with liquids or even humidity, we started investigating the possibility of covalently binding our receptors to a polymeric substrate and a patent has been deposited, in the case of ethylene vinyl alcohol (EVOH) copolymer as the starting material.[26,27] On the basis of our knowledge, this rough pathway is seldom followed in the literature and, on the contrary, several immobilization strategies have been exploited on inorganic supports,[6,13,18] filter paper,[2] and different mixtures of cellulose derivatives and polyethylene glycol (PEG).[17,19] From our point of view, covalent functionalization of the solid phase prevents any risk of dye release. Moreover, the usage of a polymeric substrate already employed in food packaging facilitates the industrial scale-up and the implementation in typical food packaging, significantly reducing the costs.

In this work, the selection of the polymeric substrate is discussed and the functionalization and pressing procedure required to obtain the final sensing material are described. Subsequently, the results of the physicochemical characterization of the polymeric films are reported, as is the application to monitoring the spoilage of real samples, with a particular focus on poultry meat and cod fillets, stored both at room temperature and in a domestic fridge. PCA was used to rationalize the array's color evolution, and the resulting models were validated by both external data set projection and independent instrumental analysis.

MATERIALS AND METHODS

All dyes were analytical reagent grade. *m*-Cresol purple (**1**), *o*-cresol red (**2**), bromothymol blue (**3**), thymol blue (**4**), chlorophenol red (**5**), and bromophenol blue (**6**) were purchased from Carlo Erba or Sigma-Aldrich.

EVOH copolymer (32% ethylene content), a 1 M thionyl chloride solution in dichloromethane, sodium hydroxide in pellets, nitric acid, ammonia, acetic acid, dimethylacetamide (DMA), and dichloromethane (DCM) were purchased from Sigma-Aldrich or Alfa Aesar.

Pictures of the array were taken by a Samsung Galaxy S7 Smartphone; a portable led light box (23 cm × 23 cm × 23 cm) was used to guarantee the reproducibility of the photos (PULUZ, Photography Light Box, Shenzhen Puluz Technology Ltd.). A picture of the box is reported in the Supporting Information.

Breast poultry meat in slices and cod fillets were bought in a local supermarket (UNES Supermarkets, via Fratelli Cervi, 11, 27100 Pavia, Italy), on the delivery day a few moments after the meat was put on the shelf.

Sensitive Part of the Sensors. Figure 1 shows the pH indicators employed in the functionalization of EVOH with their log K_a values, as found in the literature.[28−30] Compounds *m*-cresol purple (**1**), *o*-cresol red (**2**), bromothymol blue (**3**), thymol blue (**4**), and chlorophenol red (**5**) had previously been employed in the preliminary version of the array and presented in previous works.[8,24,25] In the first experiments on the polymeric material, a shift to higher log K_a values after functionalization was observed; for this reason, bromophenol blue (**6**) was added to the previous selection of dyes to investigate in a meaningful way the region below pH 7.

https://dx.doi.org/10.1021/acsfoodscitech.0c00089
ACS Food Sci. Technol. 2021, 1, 165−175

Polymeric Support of the Array. As a polymeric support, ethylene vinyl alcohol copolymers (EVOH), composed of hydrophilic (vinyl alcohol) and hydrophobic (ethylene) segments in a single macromolecule, were selected. These unique copolymers are insoluble in water and have excellent barrier properties, which made them suitable for food packaging films, especially for those foods that are sensitive to certain levels of oxygen or carbon dioxide.[31] Moreover, the presence of quite reactive hydroxyl moieties makes EVOH an excellent candidate for our purposes.[31,32]

Synthesis of Dye-EVOH@. The synthesis of the reactive polymeric material, internationally patented,[26,27] consists of two reaction steps: (i) dye activation through chlorination and (ii) polymer functionalization by nucleophilic substitution. In the first step, a selected dye is dissolved in $SOCl_2$ and the mixture is heated at reflux for 4 h; the chlorinated dye can be stored by leaving it under the $SOCl_2$ solution for ≤18 h before use. The $SOCl_2$ excess is evaporated just before the second step.

EVOH was poured in DMA at 110 °C, under stirring and a nitrogen atmosphere, and solid NaOH was added as the catalyst. When the polymer was completely dissolved, a freshly prepared sulfonyl chloride DMA solution was added dropwise to the polymer solution. After 4 h at 110 °C, the reaction mixture was cooled at room temperature and then in an ice bath.

The functionalized polymer was precipitated in cooled DCM under stirring, and the temperature was kept around 0 °C because the process is strongly exothermic; this procedure helped to increase the final yield. The solid material was then filtered under vacuum, washed with 200 mL of DCM to remove the unreacted dye excess, and left to dry overnight. A further drying step was conducted under vacuum at 60 °C for 24 h in an Abderhalden apparatus.

Pressing of the Dye-EVOH@. After the synthesis, the functionalized polymer comes in the form of small blocks of irregular shapes and needs to be pressed to obtain the final sensitive films. A dual heated plate manual press was employed, and pressing parameters were optimized by full factorial experimental design, reported in the Supporting Information. The optimized parameters are listed in Table 1.

Table 1. Optimized Parameters for Dye-EVOH@ Pressing

parameter	optimized value
polymer mass (mg)	300
pressure (psi)	2000
time (s)	30
temperature (°C)	180

Characterization of Dye-EVOH@. The physicochemical characterization was performed on different samples of each synthesized dye-EVOH@. Apart from DSC analyses, all of the other measurements were taken on the final films, obtained after pressing.

Differential scanning calorimetry (DSC) analyses were performed by heating the samples (∼5 mg) from −80 to 250 °C at a rate of 5 °C/min under a N_2 atmosphere in Al crucibles by a Q2000 instrument interfaced with a TA 5000 data station (TA Instruments). For selected samples, a second heating−cooling cycle was appended to verify the reversibility of the processes.

Fourier transform infrared (FT-IR) spectra were recorded using a Nicolet (Madison, WI) FT-IR iS10 spectrometer equipped with an attenuated total reflectance (ATR) sampling accessory (Smart iTR with a diamond plate) by co-adding 32 scans in the range from 4000 to 650 cm^{-1} with the resolution set at 4 cm^{-1}.

Elemental analyses of the films were performed by energy dispersive X-ray analysis (EDX) by an X-max 50 mm^2 probe (Oxford Instrument) connected to an EVO MA10 scanning electron microscope (SEM). The films were supported on graphite bi-adhesives fixed on Al stubs and subsequently transferred into the SEM chamber. EDX measurements were performed under ultrahigh vacuum at a working distance of 8.5 mm and with an electron generation voltage of 20 kV.

The thickness of three samples for each dye-EVOH@ film was measured by a KLA Tencor P-6 Stylus Profiler applying 2 mg force.

UV−vis spectra of dye-EVOH@ films were recorded by a Jasco V-750 spectrophotometer after equilibration for 24 h in 0.1 M HNO_3, in phosphate buffer at pH 7.00, and in 0.1 M NaOH at different pHs and compared with the corresponding spectra of the dye dissolved in aqueous solutions (∼10 μM).

Further investigations of sorption kinetics and sensitivity toward liquid and gaseous analytes are reported in the Supporting Information.

Monitoring of Real Samples. *Experimental Setup.* The dye-EVOH@ films were cut in circles of 0.5 cm diameter of approximatively 0.0025 g with a hole punch for paper to obtain the final sensors employed in the analysis of real samples. The small dimension of the sensing spot allowed us to increase the sensitivity of the sensors, as previously assumed,[8,24,25] and to obtain a homogenous sensor color, even in the presence of a low concentration of analytes.

First, the sensors were equilibrated at the proper pH by being immersed for 2 h in 10 mL of 0.01 M HNO_3 or 0.1 M NaOH on a stirring plate, these times and solutions being suitable for complete equilibration. Subsequently, the dye-EVOH@ spots were dried, placed on a stripe of Scotch 3M Magic Tape, and placed over the selling tray.

The beast poultry meat and cod fillets were purchased in a local supermarket. We bought directly ready trays made of a plastic container (PP) for food and covered with a low-permeability polyethylene plastic film. Trays containing around 300 g for poultry meat and 200 g for cod fillets were used, being the most common quantity in this kind of packaging. The trays were taken from the shelf, a few minutes after the preparation to ensure a homogeneous lifetime of all samples. Within 10 min, the samples were in the lab, the plastic film was removed, the stripes with sensors were placed over the tray, and a new plastic film was fixed around the tray. The samples were stored at room temperature, under the hood, or in the fridge (4 °C), depending on the type of experiment.

The same procedure was applied for the analysis of both protein foods except for the preliminary equilibration step: for chicken meat samples, dyes **1**−**5** were dipped in a basic solution and only dye **6** was immersed in an acidic solution; for fish samples, dye **5** was previously equilibrated at acidic pH.

Color Analysis and Chemometrics. At given times, during storage at different temperatures, trays were placed in a lightbox, to ensure constant illumination conditions, and photos of the array were acquired. For each sensor in the array, RGB triplets were collected using GIMP software[33] and employed for data treatment. The RGB space color was preferred over others because the RGB indexes can better describe shade modification and color changes than other parameters.

Then, principal component analysis (PCA) was performed on RGB triplets, only centering the data because these indexes are intrinsically scaled from 0 to 255, to model the degradation process. More advanced chemometric techniques could be employed in such analyses, but our aim was just to rationalize the color evolution and visualize the process; PCA was suitable for these purposes. The open-source program CAT (Chemometric Agile Tool)[34] was employed.

Training Set. For each protein food, two trays were purchased and used to monitor the spoilage process, as described previously, at room temperature (around 22 °C).

Validation by an External Test Set and Instrumental Analysis. Then, for each food, two new samples were analyzed. For each sample, almost the entire quantity was left in the tray with the array and kept as a reference, while the rest was divided into subsamples for instrumental analyses. At a given time, the array was photographed, and the content of two vials was subjected to analysis of the headspace and the solid, as described below. The RGB data acquired from the photo were projected as an external data set in the PCA model to verify the correct allocation of the samples, while the information about the composition of the solid and the headspace was employed to confirm the results shown by PCA.

To corroborate the assumptions derived from PCA, we performed instrumental analysis on samples of chicken and cod at different degradation steps. Each analysis was performed in triplicate, and each sample split into two parts, one for the solid analysis and one for the identification of the volatile in the headspace. All of the analyses were

https://dx.doi.org/10.1021/acsfoodscitech.0c00089
ACS Food Sci. Technol. 2021, 1, 165−175

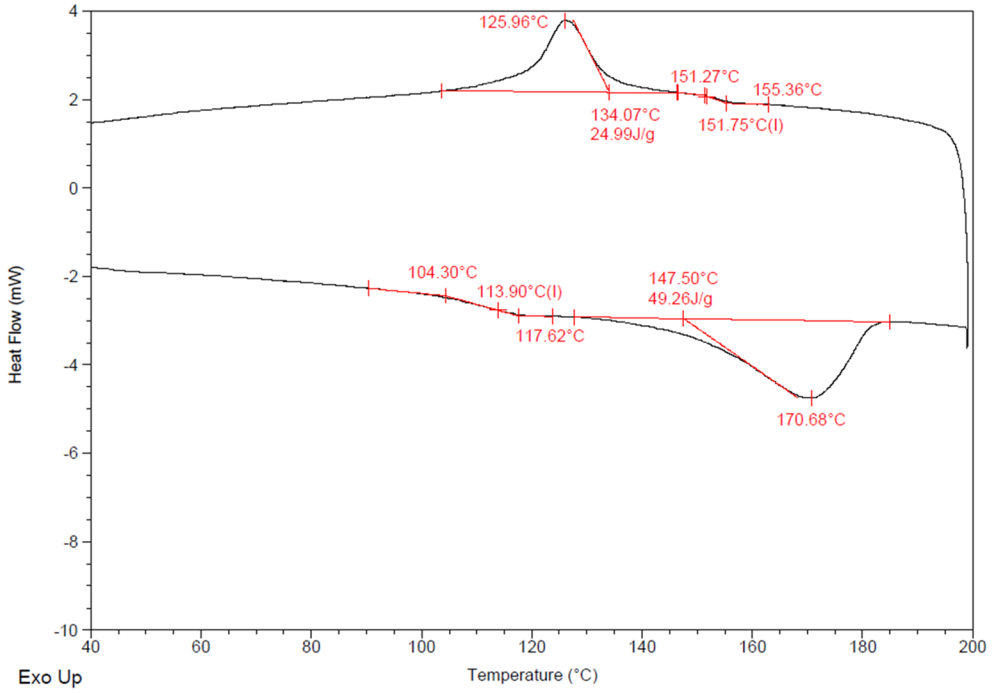

Figure 2. DSC curve of **3**-EVOH@.

performed at CGS (Centro Grandi Strumenti), which is one of the facilities of the University of Pavia.

For the analysis of the solid, we followed the procedure suggested in the literature.[35,36] In the case of chicken meat, each piece of meat was cut in a blender, and 4 g was extracted with an Ultra-Turrax S 18N-10G homogenizer (IKA-Werke Gmbh & Co.) and 5% TCA and then centrifuged. On the contrary, for cod fillets, the first part of the procedure was slightly modified to improve amine extraction. Twenty grams was chopped, using a common kitchen mixer, left to equilibrate in 20 mL of 10% TCA at the proper temperature, and centrifuged. For both protein foods, after the centrifugation step, the supernatants were collected and purified on SPE STRATA X cartridges (conditioned with 4 mL of methanol followed by 4 mL of Milli-Q water). Then, 2 mL of the sample (supernatant), with a pH adjusted to around 11 upon addition of 200 μL of 28% NH_4OH, was passed through the cartridges. After sample loading had reached completion, cartridges were rinsed with 2 mL of a MeOH/H_2O mixture [5:95 (v/v)] and dried under vacuum to remove the excess of water. Analytes were eluted from the STRATA X sorbents with 2 + 2 mL of a solution of a methanol/acetic acid mixture [99:1 (v/v)]. The eluting solution was dried with nitrogen gas, and the residue collected with 2 mL of 0.1 M HCl, filtered, and injected into the LC-MS/MS instrument.

On the contrary, for volatile analysis, samples (~5 g) were placed in the vials equipped with the solid phase, kept under the same storage conditions of samples, and then analyzed by LC-MS/MS. The analyses were performed directly using headspace solid phase microextraction (HSSPME) coupled with gas chromatography and mass spectrometry (GC/MS). The following experimental parameters were used: polydimethylsiloxane/divinylbenzene (PDMS/DVB) fiber, 65 μm; extraction temperature, 35 °C; extraction time, 20 min; desorption temperature, 250 °C; desorption time, 4 min. GC/MS analysis was performed on a Thermo Scientific DSQII single-quadrupole GC/MS system (Thermo Fisher Scientific, Milan, Italy) equipped with a Restek Rtx-5 MS capillary column [30 m, 0.25 mm (inside diameter), 0.25 μm film thickness], with helium as the carrier gas at a constant flow rate of 1.0 mL/min. The injector temperature was set at 250 °C, and the injector was operated in splitless mode. The oven was held at 35 °C for 2 min, and then the temperature was increased to 80 °C at a rate of 5 °C/min, ramped to 300 °C at a rate of 10 °C/min, and finally held at 300 °C for 2 min. The GC transfer line temperature was 270 °C. All mass spectra were acquired in electron impact mode (ionization energy of 70 eV and source temperature of 250 °C), with spectra acquired in full scan mode (mass range of m/z 15−650 and scan speed of 832 amu/s). Assignment of chemical structures to chromatographic peaks was based on the comparison with the databases for the GC/MS NIST Mass Spectral Library (NIST 08) and the Wiley Registry of Mass Spectral Data (8th edition). Xcalibur MS Software version 2.1 (Thermo Scientific Inc.) and the AMDIS Program for the automated deconvolution of mass spectra were used for GC/MS data interpretation.

RESULTS AND DISCUSSION

Synthesis and Characterization of Dye-EVOH@. The same synthesis was successfully performed for all of the dyes, and no differences were observed among the dyes. Moreover, yields were sufficiently high for our purpose in all of the syntheses, with >4.5 g of the functionalized polymer obtained after the last drying step.

At first, DSC analyses were performed on the irregular blocks obtained after the synthesis. Figure 2 shows, as an example, the DSC curve of **3**-EVOH@, and the other profiles are reported in the Supporting Information.

The calorimetric profile showed for all of the samples, after a second order transition (evident for only some of them), an endothermic melting peak (onset temperature of 147.50 °C and peak temperature of 170.68 °C for **3**-EVOH@ in Figure 2) upon being heated. The process was fully reversible, as evidenced in the cooling part of the calorimetric curve. In Table 2, the onset and peak temperature for the melting process of all of the investigated polymeric materials are reported.

The remaining part of the characterization was performed on the films obtained after pressing (see the procedure described in Pressing of the Dye-EVOH@).

At first, the film thickness was measured multiple times on samples functionalized with different receptors. This physical parameter was crucial in the development of new sensors. On one hand, thinner sensors ensure both higher sensitivity and homogeneity in color shade and color changes. On the other

https://dx.doi.org/10.1021/acsfoodscitech.0c00089
ACS Food Sci. Technol. 2021, 1, 165−175

Table 2. Onset and Peak Temperatures for the Melting of Functionalized Polymers

functionalized polymer	receptor	onset temperature (°C)	peak temperature (°C)
1-EVOH@	*m*-cresol purple	125.69	152.17
2-EVOH@	*o*-cresol red	152.00	170.16
3-EVOH@	bromothymol blue	147.50	170.68
4-EVOH@	thymol blue	137.85	160.19
5-EVOH@	chlorophenol red	148.74	168.43
6-EVOH@	bromophenol blue	145.59	167.97

hand, the thickness must be reproducible to guarantee the same sensing performances for all of the spots and to minimize the differences among the sensors. From these measurements, we observed that no significant differences were highlighted, in films containing different pH indicators, and 168(11) μm was found to be the medium thickness value. This result is satisfying in terms of both thickness and reproducibility.

Then, the FT-IR spectra of the pH indicator powders, starting EVOH copolymer, and functionalized films were recorded and compared. In Figure 3, the results for bromothymol blue (**3**) are shown while the spectra for the other pH indicators are reported in the Supporting Information.

The same signals characterized the spectra of EVOH before and after the functionalization (Figure 3b,c); the only difference was the presence of a band at 1615 cm^{-1}, due to the formation of a sulfonic ester from the reaction between the receptor's sulfonic group, previously activated, and the polymer's hydroxyl group, demonstrating the successful modification of the starting material.

Lastly, electron images of the films were acquired, and elementary analysis was performed. In Figure 4, the SEM images acquired on the surface of the polymeric film at increasing magnitudes, in secondary electron mode, and the results of EDX analysis are displayed in the case of **3**-EVOH@.

The SEM images show a compact and homogeneous surface, with no pores and no holes on it, while from the elemental analysis, it was possible to evidence the presence of S in the sample. Because S is present only in the receptor's structure, from the atomic percent of this element (~0.3%) we were able to estimate the millimoles of the receptor, successfully bonded to the polymer matrix, per sensor (~0.2 μmol per spot of 0.5 cm diameter). Because the weight of one spot is ~2.5 mg, this means an estimated capacity of 0.1 mmol/g.

UV−Vis Characterization of Dye-EVOH@. The optical behavior of these new reactive materials was first investigated by UV−vis spectroscopy. The sensing spots, prepared to monitor real samples, are too small for this test, so 2 cm × 2.5 cm rectangles were cut and employed instead. For each receptor under investigation, we wanted to compare the optical behavior of the molecule in aqueous solution and after functionalization at different pH values. In Figure 5, the results for bromothymol blue (**3**) are displayed: UV−vis spectra and corresponding photographs of 9.5 μM aqueous solutions of **3** and **3**-EVOH@, after equilibration at acidic, basic, and neutral pH, as described in Materials and Methods.

Many conclusions could be drawn from these experiments. First, the maximum of the absorbance band, for acid and alkaline forms of the indicator, was located at a very similar wavelength in solution and films (λ_{max} = 433 and 430 nm, respectively, for the acid species, and λ_{max} = 617 and 628 nm, respectively, for the alkaline species), and only a small shift was observed. Consequently, from naked-eye analysis of the photographs, the colors of solutions and films were similar at extremely acidic and alkaline pHs. Obviously, the spectra presented a different absorbance value at the maximum due to the different amount of dye in the solution and film, but this was not relevant for the qualitative investigation of the optical behavior of the polymers.

As for the samples in phosphate buffer, a pH value of ~7 was chosen because the log K_a in a solution of this pH indicator is 7.1.[28,30] For this reason, in the solution spectra, both the absorbance bands of acidic and alkaline forms were visible, with similar heights, and in the photograph, a mixture of the yellow acid form and the blue alkaline form resulted in a dark green shade. A completely different behavior was observed for the functionalized polymer: the main absorbance peak is the one related to the acidic form, while the peak at 628 nm was not even visible and, indeed, the sensing film is completely yellow. Because, after the preparation, a sufficiently long time was set to ensure the equilibration of the reactive material with the buffered solution, the only possible explanation for this behavior is that, together with the functionalization, a shift toward higher log K_a values occurs. The same behavior was observed, performing similar analysis for all of the indicators under investigation (see the Supporting Information), and a shift of more than one unit could be hypothesized, in good agreement with similar data acquired by other research groups.[37−40] Undoubtedly, a more precise determination of log K_a values after functionalization could be performed, but this is outside the scope of this work. Nevertheless, to understand which sensors are more useful for following the spoilage process, a rough estimate of this shift must be undertaken, which will be shown below.

Monitoring of Real Samples. *Evolution of the Colors over Chicken Meat.* Having equilibrated the sensing spots at the proper pH value and having prepared the samples, as reported in Materials and Methods, we registered the evolution of the array color over trays of breast poultry meat. In Figure 6a, an example of color evolution is reported.

In the first part of the degradation process, the receptors with log K_a values of >7 (dyes **1**−**4**), previously equilibrated at basic pH, partially turned to the acid form due to the reaction with acid volatiles released by bacteria. Then, in the second part of the spoilage process, the pH of the headspace underwent a slight increase, due to the end of acid production and the formation of amines in the meat, and thus, the receptor with the lowest log K_a value, dye **6**, turned into the blue basic form. As one can easily observe in the photographs, dye **5** turned out to be unreactive and therefore useless in spoilage monitoring of chicken samples and could be discarded for a future large-scale implementation.

PCA was then performed on the RGB triplets of the sensors during degradation. Analyzing the score plot reported in Figure 6b, we noticed that the score value on PC1, which accounts for 61.80% variability, increased during time and could be correlated to degradation while PC2 accounted for the variability among samples. Moreover, three different clusters, called SAFE, WARNING, and HAZARD, could be identified, with widely different values on PC1, and a similar behavior was also observed upon storage of the samples at 4 °C; however, the time line of the spoilage was greatly increased.

Evolution of the Colors over Cod Fillets. As for chicken meat, also for cod fillets, the standard procedure, described in Materials and Methods, was followed, and photos of the array were taken

https://dx.doi.org/10.1021/acsfoodscitech.0c00089
ACS Food Sci. Technol. 2021, 1, 165−175

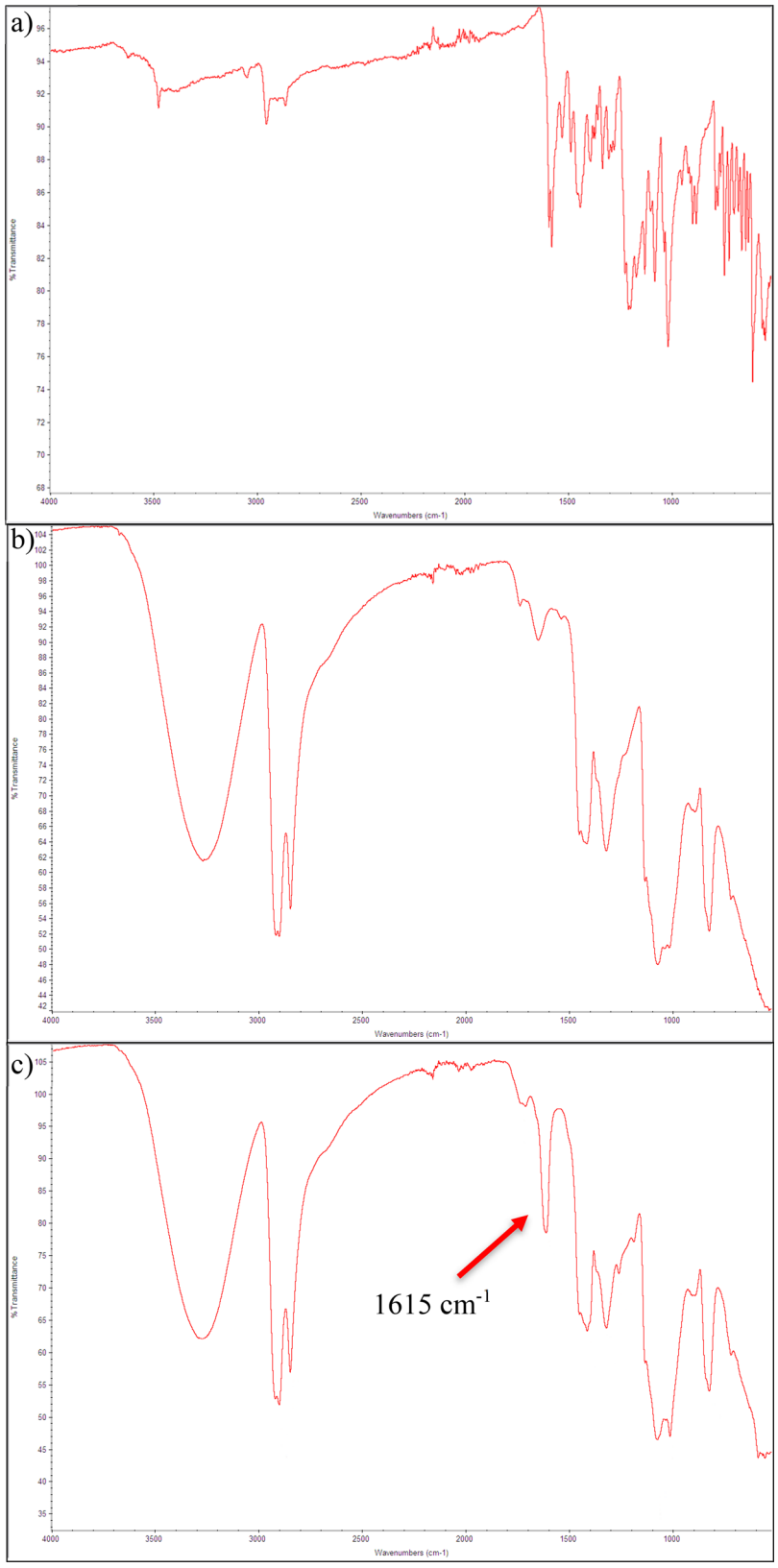

Figure 3. FT-IR spectra of (a) bromothymol blue powder, (b) EVOH copolymer, and (c) functionalized polymeric film **3**-EVOH@.

during the degradation process. In Figure 7a, the color evolution of the array is reported.

The behavior of the sensing units is very similar to that observed in the case of chicken meat. At first, receptors with log K_a values of >7 (dyes **1**−**4**) partially turned to the acid form revealing the presence of acid volatile byproducts in the headspace. After 21 h, dye **6** started to react and turn to the blue basic form but, compared to poultry meat monitoring, the reaction was faster, and a complete conversion was observed. Moreover, dye **5**, with a log K_a value of 6.1 in solution, partially

https://dx.doi.org/10.1021/acsfoodscitech.0c00089
ACS Food Sci. Technol. 2021, 1, 165−175

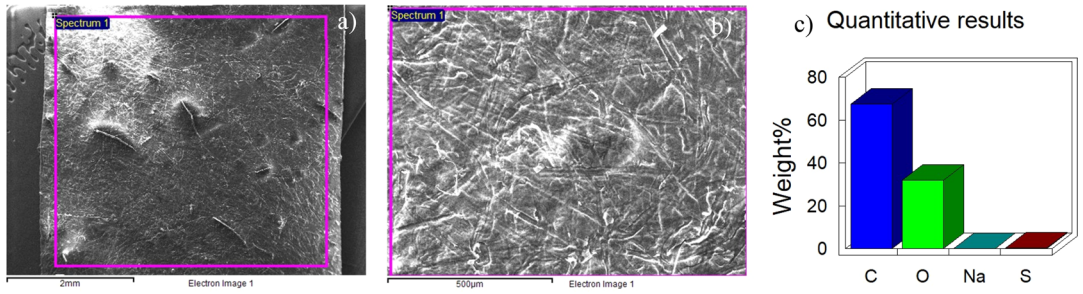

Figure 4. (a and b) SEM images of **3**-EVOH@ at different magnifications and (c) quantitative results of elemental analysis of **3**-EVOH@.

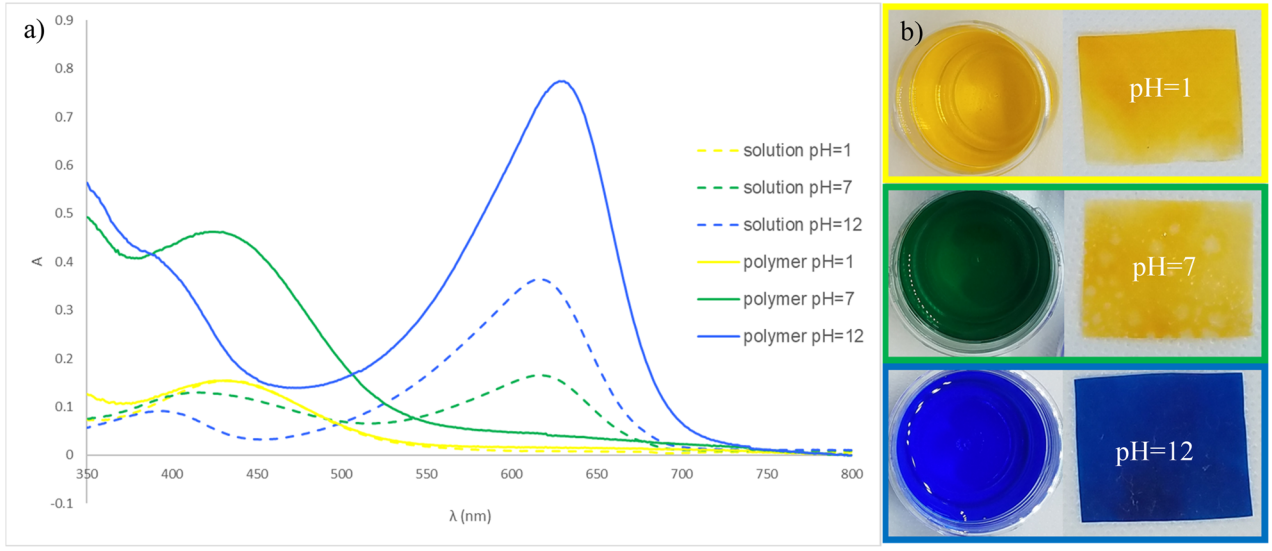

Figure 5. (a) UV−vis spectra and (b) corresponding photographs of a 9.5 μM bromothymol blue (**3**) solution (dashed lines) and **3**-EVOH@ (solid lines) after equilibration at pH 1 (yellow), 7 (green), and 12 (blue).

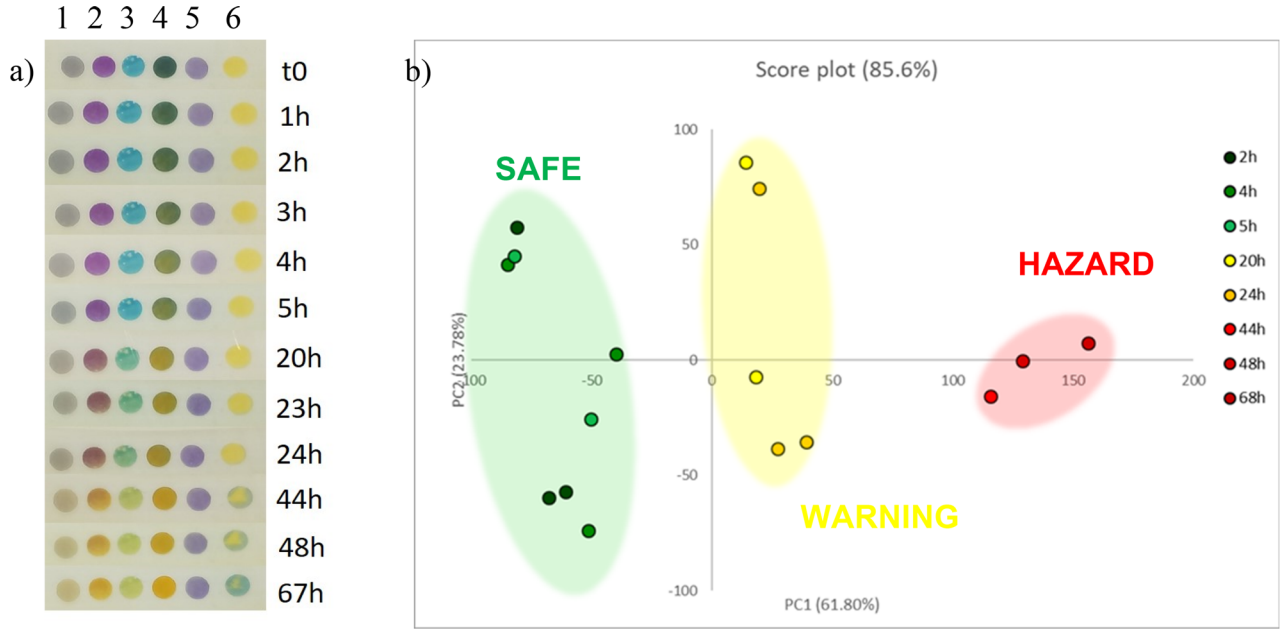

Figure 6. (a) Evolution of the sensing spots on one sample of poultry meat and (b) plot of the scores of the PCA model on the first two principal components. The green, yellow, and red shaded areas indicating samples defined as SAFE, WARNING, and HAZARD, respectively, are exclusively added as a simplification of the different groups.

turned to the basic color in the last monitoring hours. This means that the resulting pH in the headspace was higher in the case of fish than in the case of chicken, and the spoilage process of this food is much faster, according to common knowledge.

https://dx.doi.org/10.1021/acsfoodscitech.0c00089
ACS Food Sci. Technol. 2021, 1, 165−175

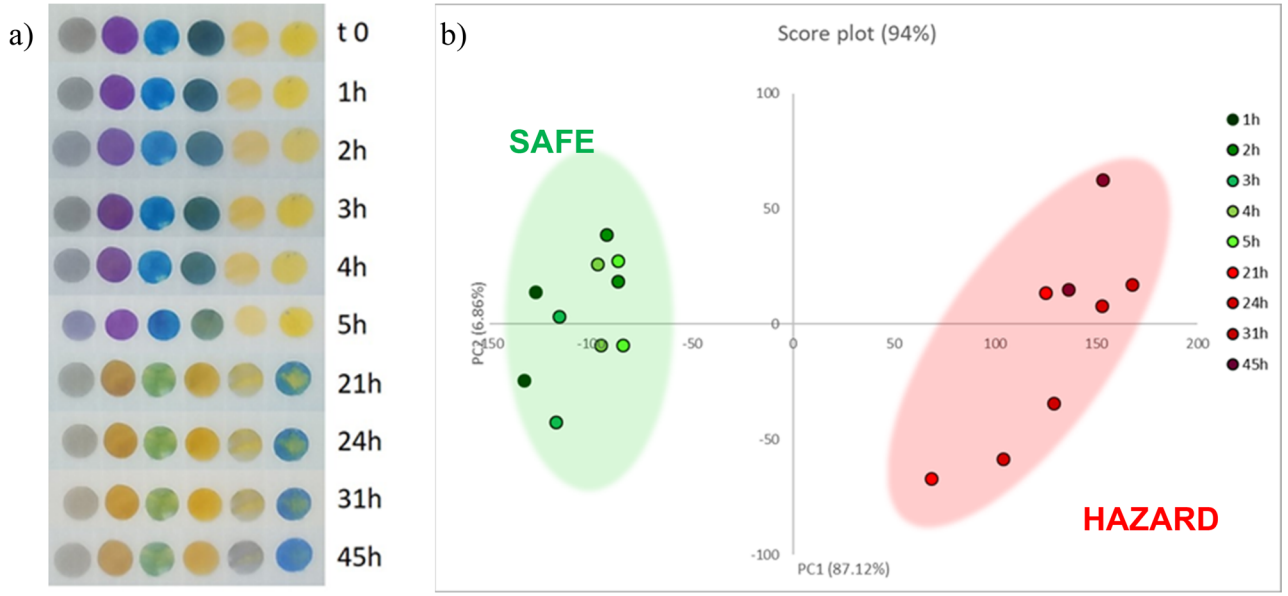

Figure 7. (a) Evolution of the sensing spots on one sample of cod fillets and (b) plot of the scores of the PCA model on the first two principal components. The green, yellow, and red shaded areas indicating samples defined as SAFE, WARNING, and HAZARD, respectively, are exclusively added as a simplification of the different groups.

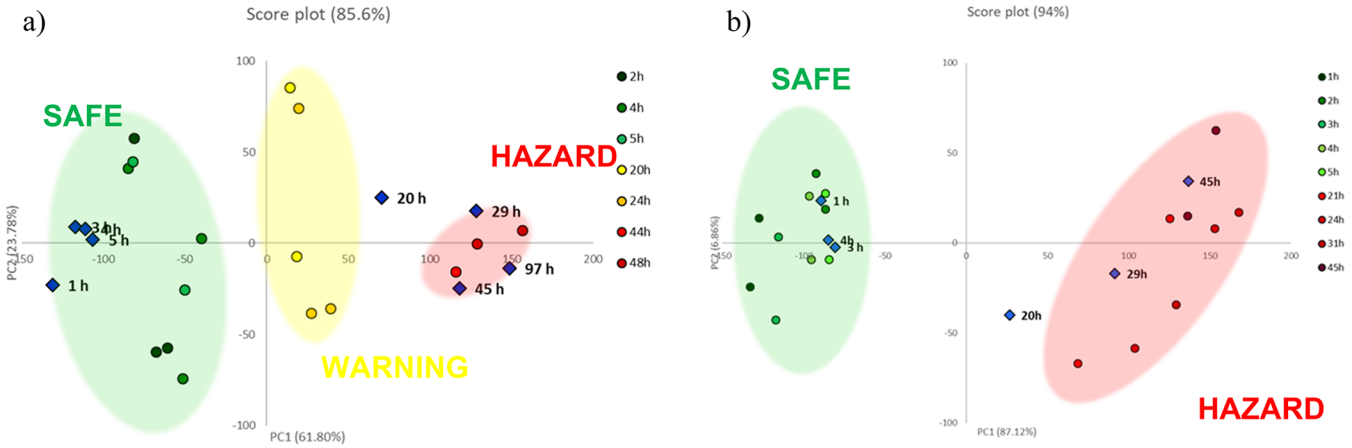

Figure 8. Projection of the external data set in the plot of scores of the first two components for (a) chicken meat and (b) cod fillets.

Nevertheless, even in the case of fish, we cannot consider the pH of the headspace "basic" because the other receptors, with slightly higher pK_a values, remained in the acid form. This assumption was then confirmed by the instrumental analysis reported below.

Eventually, PCA was used to display the degradation of cod samples and the resulting plot of scores is shown in Figure 7b. PC1 (87.12% variability) was correlated with the spoilage process, and PC2 (6.86% variability) with the differences between the samples analyzed. On PC1, two well-separated clusters, called SAFE and HAZARD, could be identified, upon storage of the samples at room temperature, while three clusters were observed for the samples kept at 4 °C. This difference was due to the high perishability of fish. At room temperature, one night was enough to observe the complete spoilage of the food, while at 4 °C, the intermediate step could also be observed.

For both chicken and fish samples, these analyses were a proof of concept to demonstrate that the polymer-based device described here can be employed in food freshness monitoring because the color evolution observed is in line with CSI and volatile byproducts released during spoilage and, even more importantly, with the composition of the solid and headspace, as described below. To develop a complete model, more samples are required and other chemometric tools are preferred, but this kind of analysis would be performed only using the fully developed device.

Validation by an External Data Set and Instrumental Analysis. For each food, new samples were used to verify the degradation pathway displayed by PCA. As previously described, these validation samples were divided into three parts. Almost the entire amount of meat or fish was sealed in a tray and analyzed using the array of sensors, following the same procedure used in the previous analysis; a small amount was used for extraction and identification of BA by LC-MS/MS, and the remaining part was placed in vials and employed in the analysis of the headspace composition using HSSPME coupled with GC/MS. We aimed to demonstrate that new samples were still located in the right clusters by PCA and that the clusters were not artifacts, but they were characterized by significant differences in the solid and headspace composition.

https://dx.doi.org/10.1021/acsfoodscitech.0c00089
ACS Food Sci. Technol. 2021, 1, 165−175

Table 3. Identification of BA in Chicken Meat, Performed through HPLC-ESI/MS Analysis, Corresponding to the Three Degradation Steps Identified by PCA, S (safe), W (warning), and H (hazard)

BA	precursor ion	S	pick area S	W	pick area W	H	pick area H
spermidine	146	no	–	yes	573723	yes	558980
cadaverine	103	no	–	no	–	yes	199409
putrescine	89	no	–	no	–	yes	13577
histamine	112	no	–	yes	38082	yes	37320
spermine	203	no	–	yes	55085	yes	45372
tyramine	138	no	–	no	–	yes	254478
2-phenylethylamine	122	no	–	yes	32923	yes	30311

As for the projection in the PCA model, in Figure 8 plots of scores of chicken meat and cod fillets after the projection of the test set are shown.

At first glance, we notice that new samples showed the same degradation pathway of the training set and were located in the right clusters. As previously mentioned, in strict terms, these cannot be considered real validated models of degradation due to the very small number of samples, both in the training and in the test set, but they are promising results for this first proof of concept and, above all, this first screening was useful for identifying the clusters that had to be characterized by instrumental analysis.

As for the analysis of the solid, the results are displayed in Table 3, in the case of chicken meat, and Table 4, in the case of cod fillets.

Table 4. Identification of BA Performed in Cod Fillets through HPLC-ESI/MS Analysis Corresponding to the Two Degradation Steps Identified by PCA, S (safe) and H (hazard)

BA	precursor ion	S	pick area S	H	pick area H
spermidine	146	yes	13079	yes	28800
cadaverine	103	yes	31739	yes	62863
putrescine	89	no	–	no	–
histamine	112	yes	8993	yes	40463
spermine	203	yes	12111	yes	34185
tyramine	138	no	–	yes	19399
2-phenylethylamine	122	yes	53750	yes	68334
tryptamine	161	yes	52519	yes	63562

For chicken meat, qualitative identification of BAs present in the solid was enough to clearly distinguish the samples belonging to different clusters. In the SAFE zone, no amines were detected; in the WARNING zone, four of seven were found, while all of the BAs under investigation were detected in the HAZARD zone. On the contrary, in the case of cod fillets, almost all of the BAs can be detected even in the SAFE zone. It is well known that fish samples contain a large number of amines, even when it is fresh, and even the fishy odor is due to volatile amines, in particular trimethylamine. Moreover, this food is highly perishable, and for this reason, the production of BA is very fast and significant even in the small time required for the analysis. Nevertheless, a substantial difference between the SAFE and HAZARD zones in the amount of BA was detected: apart from 2-phenylethylamine and tryptamine, from the pick areas we noticed that the entire quantity of each amine was at least double, or even more, in the HAZARD zone rather than in the SAFE one. We decided not to quantify these molecules in the solid because our aim was not to fully characterize the composition of cod fillets during the spoilage process but just to demonstrate that the clusters, recognized by our array of sensors, are reflected in and confirmed by different compositions of samples and headspace.

Eventually, the headspace composition was analyzed, and the results are reported below in Tables 5 and 6.

Table 5. Identification of the Class of Substances Detected in the Headspace of Chicken Meat, Performed through HPLC-ESI/MS Analysis, Corresponding to the Three Degradation Steps Identified by PCA, S (safe), W (warning), and H (hazard)

	S	W	H
alcohols	√	√	√
aldehydes	√	√	√
ethanol	√	√	√
acids	√	√	√
ketones	–	√	√
esters	–	√	√
thiols	–	√	√
biogenic amines	–	–	–
indole	–	–	√

Table 6. Identification of the Class of Substances Detected in the Headspace of Cod Fillets, Performed through HPLC-ESI/MS Analysis, Corresponding to the Two Degradation Steps Identified by PCA, S (safe) and H (hazard)

	S	H
alcohols	√	√
aldehydes	√	√
ethanol	√	√
acids	√	√
ketones	√	√
esters	√	√
thiols	√	√
trimethylamine	√	√
volatile amines	–	√
biogenic amines	–	–
indole	–	√

Also for headspace analysis, the case of chicken meat was easier to interpret and deal with because in the SAFE zone very few classes were detected and, above all, a large number of acid compounds were found, as suggested by the color evolution of the array of sensors. In the WARNING zone, ketones and esters were released after the bacterial catabolism of sugars and their derivatives, but no amines were detected even if, at this stage, they were present in the meat, as described in the preceding paragraph. In the HAZARD cluster, when all of the BAs were

https://dx.doi.org/10.1021/acsfoodscitech.0c00089
ACS Food Sci. Technol. 2021, 1, 165−175

detected in large amounts in the solid, amines were not found in the headspace, confirming our previous assumption about this topic.[24,25] The main qualitative difference between these two last clusters was the presence of indole in the HAZARD zone.

As for cod fillets, the composition of the headspace in the two clusters was very similar and, as previously argued, trimethylamine was present in both samples, but important details were nevertheless observed. At first, small volatile amines were present only in the HAZARD step but BAs were again never detected; second, indole was revealed in the second part of the degradation process, which was similar to what was observed in chicken meat samples.

In conclusion, the instrumental analysis of the headspace during degradation confirmed not only the behavior of our sensors but also all of the previous assumptions. BA were produced, even in large quantities, in the solid when food is no longer eatable, but due to the buffered pH of the solid phase, they were present in their protonated form so they did not fly and, consequently, could not be detected in the headspace at any step. Therefore, only a very slight increase in the headspace pH was observed and, in fact, only the receptor with a very low log K_a value showed a complete reaction to the basic form due to the reduction on acid volatile byproducts released or, only for fish samples, to the presence of small volatile amines.

Further Developments. We confirmed the applicability of the optode toward protein food degradation monitoring by naked-eye evaluation and spoilage modeling by PCA on RGB triplets. Furthermore, the degradation pathway visualized by PCA and the location of unknown samples were confirmed by independent instrumental analyses, performed both on food and on the headspace to identify the different compositions during spoilage. These promising results suggested us to test the applicability of the optode with different protein foods and to reduce the number of sensors employed to the most significant ones.

The final aim would be the development of a dual-sensor device that can recognize all of the degradation steps, suitable for naked-eye freshness evaluation for a large variety of protein foods. Also, the goals already achieved, like low cost, easy implementation in food packaging, and the absence of dye leaching, would be maintained.

■ ASSOCIATED CONTENT

Supporting Information

The Supporting Information is available free of charge at https://pubs.acs.org/doi/10.1021/acsfoodscitech.0c00089.

Description of the light box (section 1S), experimental design for pressing procedure optimization (section 2S), DSC curves (section 3S), IR spectra (section 4S), and UV−vis spectra (section 5S) of dye-EVOH@ not included in the text, analytical characterization of sensing performances of the array in liquid samples as 0.01 M HNO_3 (section 6S), 0.1 M NaOH (section 7S), phosphate buffer at pH 7 (section 8S), and gaseous samples as acetic acid (section 9S) and ammonia (section 10S) at different concentrations, and a stability test upon exposure to phosphate buffer at pH 7 (section 11S) (PDF)

■ AUTHOR INFORMATION

Corresponding Author

Lisa Rita Magnaghi − *Department of Chemistry, University of Pavia, 27100 Pavia, Italy; Unità di Ricerca di Pavia INSTM, 50121 Firenze, Italy;* orcid.org/0000-0002-4484-4788; Email: lisarita.magnaghi01@universitadipavia.it

Authors

Giancarla Alberti − *Department of Chemistry, University of Pavia, 27100 Pavia, Italy*

Chiara Milanese − *Department of Chemistry, University of Pavia, 27100 Pavia, Italy*

Paolo Quadrelli − *Department of Chemistry, University of Pavia, 27100 Pavia, Italy; Unità di Ricerca di Pavia INSTM, 50121 Firenze, Italy;* orcid.org/0000-0001-5369-9140

Raffaela Biesuz − *Department of Chemistry, University of Pavia, 27100 Pavia, Italy; Unità di Ricerca di Pavia INSTM, 50121 Firenze, Italy;* orcid.org/0000-0002-2192-5032

Complete contact information is available at: https://pubs.acs.org/10.1021/acsfoodscitech.0c00089

Author Contributions

Conceptualization: R.B., P.Q., and L.R.M. Formal analysis: L.R.M. Physicochemical characterization: C.M. Funding acquisition: P.Q. Writing of the original draft: L.R.M. Review and editing: G.A., L.R.M., and R.B. Investigation: L.R.M. and P.Q. Supervision, R.B. All authors have read and agreed to the published version of the manuscript.

Notes

The authors declare no competing financial interest.

■ ACKNOWLEDGMENTS

The authors thank MIUR for funding Lisa Rita Magnaghi's Ph.D. grants and the "VIPCAT - Value Added Innovative Protocols for Catalytic Transformations" project (CUP: E46D17000110009) for valuable financial support.

■ ABBREVIATIONS USED

BA, biogenic amines; CSI, chemical spoilage index; CC, Color Catcher; EVOH, ethylene vinyl alcohol; PEG, polyethylene glycol; DMA, dimethylacetamide; DCM, dichloromethane; DSC, differential scanning calorimetry; FT-IR, Fourier transform infrared spectroscopy; ATR, attenuated total reflectance; EDX, energy dispersive X-ray analysis; SEM, scanning electron microscope; HSL/HSB, hue, saturation, lightness/hue, saturation, brightness; PCA, principal component analysis; RT, room temperature

■ REFERENCES

(1) Dainty, R.H. Chemical/biochemical detection of spoilage. *Int. J. Food Microbiol.* **1996**, *33*, 19−33.

(2) Kuswandi, M.; Nurfawaidi, A. On-package dual sensors label based on pH indicators for real-time monitoring of beef freshness. *Food Control* **2017**, *82*, 91−100.

(3) Nychas, G.-J. E.; Tassou, C. C. Spoilage process and proteolysis in chicken as detected by HPLC. *J. Sci. Food Agric.* **1997**, *74*, 199−208.

(4) Nychas, G.-J. E.; Skandamis, P. N.; Tassou, C. C.; Koutsoumanis, K. P. Meat spoilage during distribution. *Meat Sci.* **2008**, *78*, 77−89.

(5) Casaburi, A.; Piombino, P.; Nychas, G.-J. E.; Villani, F.; Ercolini, D. Bacterial populations and volatilome associated to meat spoilage. *Food Microbiol.* **2015**, *45*, 83−102.

(6) Chen, Q.; Hui, Z.; Zhao, J.; Ouyang, Q. Evaluation of chicken freshness using low-cost colorimetric sensor array with AdaBoost-

OLDA classification algorithm. *LWT-Food Sci. Technol.* **2014**, *57*, 502−507.
(7) Wojnowski, W.; Majchrzak, T.; Dymerski, T.; Gebicki, J.; Namiesnik, J. Electronic noses: Powerful tools in meat quality assessment. *Meat Sci.* **2017**, *131*, 119−131.
(8) Magnaghi, L. R.; Capone, F.; Zanoni, C.; Alberti, G.; Quadrelli, P.; Biesuz, R. Colorimetric sensor array for monitoring, modelling and comparing spoilage processes of different meat and fish foods. *Foods* **2020**, *9*, 684.
(9) Alonso-Lomillo, M. A.; Domìnguez-Renedo, O.; Matos, P.; Arcos-Martìnez, M. J. Disposable biosensors for determination of biogenic amines. *Anal. Chim. Acta* **2010**, *665*, 26−31.
(10) Henao-Escobar, W.; Dominguez-Renedo, O.; Asuncion Alonso-Lomillo, M.; Julia Arcos-Martinez, M. Simultaneous determination of cadaverine and putrescine using a disposable monoamine oxidase based biosensor. *Talanta* **2013**, *117*, 405−411.
(11) Papadopoulou, O. S.; Panagou, E. Z.; Mohareb, F. R.; Nychas, G.-J. E. Sensory and microbiological quality assessment of beef fillets using a portable electronic nose in tandem with support vector machine analysis. *Food Res. Int.* **2013**, *50*, 241−249.
(12) Salinas, Y.; Ros-Lis, J. V.; Vivancos, J. L.; Martinez-Manez, R.; Marcos, M. D.; Aucejo, S.; Herranz, N.; Lorente, I. Monitoring of chicken meat freshness by means of a colorimetric sensor array. *Analyst* **2012**, *137*, 3635−3643.
(13) Salinas, Y.; Ros-Lis, J. V.; Vivancos, J. L.; Martinez-Manez, R.; Marcos, M. D.; Aucejo, S.; Herranz, N.; Lorente, I.; Garcia, E. A novel colometric sensor array for monitoring fresh pork sausages. *Food Control* **2014**, *35*, 166−176.
(14) Salinas, Y.; Ros-Lis, J. V.; Vivancos, J. L.; Martinez-Manez, R.; Aucejo, S.; Herranz, N.; Lorente, I.; Garcia, E. A chromogenic sensor array for boiled marinated turkey freshness monitoring. *Sens. Actuators, B* **2014**, *190*, 326−333.
(15) Zaragoza, P.; Fernandez-Segovia, I.; Fuentes, A.; Vivancos, J. L.; Ros-Lis, J. V.; Barat, J. M.; Martinez-Manez, R. Monitorization of Atlantic salmon (Salmo salar) spoilage using an optoelectronic nose. *Sens. Actuators, B* **2014**, *195*, 478−485.
(16) Chun, H.; Kim, B.; Shin, H. Evaluation of a freshness indicator for quality of fish products during storage. *Food Sci. Biotechnol.* **2014**, *23*, 1719−1725.
(17) Rukchon, C.; Nopwinyuwong, A.; Trevanich, S.; Jinkarn, T.; Suppakul, P. Development of a food spoilage indicator for monitoring freshness of skinless chicken breast. *Talanta* **2014**, *130*, 547−554.
(18) Urmila, K.; Li, H.; Chen, Q.; Hui, Z.; Zhao, J. Quantifying of total volatile basic nitrogen (TVB-N) content in chicken using a colorimetric sensor array and nonlinear regression tool. *Anal. Methods* **2015**, *7*, 5682−5688.
(19) Chen, H.; Zhang, M.; Bhandari, B.; Yang, C. Development of a novel colorimetric food package label for monitoring lean pork freshness. *LWT-Food Sci. Technol.* **2019**, *99*, 43−49.
(20) Valdez, M.; Gupta, S. K.; Lozano, K.; Mao, Y. ForceSpun polydiacetylene nanofibers as colorimetric sensor for food spoilage detection. *Sens. Actuators, B* **2019**, *297*, 126734.
(21) Zhang, H.; Hou, A.; Xie, K.; Gao, A. Smart color-changing paper packaging sensors with pH sensitive chromophores based on azo-anthraquinone reactive dyes. *Sens. Actuators, B* **2019**, *286*, 362−369.
(22) MikŠ-Krajnik, M.; Yoon, Y.-J.; Yuk, H.-G. Detection of volatile organic compounds as markers of chicken breast spoilage using HS-SPME-GC/MS-FASST. *Food Sci. Biotechnol.* **2015**, *24*, 361−372.
(23) MikŠ-Krajnik, M.; Yoon, Y.-J.; Ukuku, D.O.; Yuk, H.-G. Identification and Quantification of Volatile Chemical Spoilage Indexes Associated with Bacterial Growth Dynamics in Aerobically Stored Chicken. *J. Food Sci.* **2016**, *81*, M2006−M2014.
(24) Magnaghi, L. R.; Alberti, G.; Capone, F.; Zanoni, C.; Mannucci, B.; Quadrelli, P.; Biesuz, R. Development of a dyes-based device to assess the poultry meat spoilage. Part II: array on act. *J. Agric. Food Chem.* **2020**, *68*, 12710−12718.
(25) Magnaghi, L. R.; Alberti, G.; Quadrelli, P.; Biesuz, R. Development of a dye-based device to assess the poultry meat spoilage. Part I: building and testing the sensitive array. *J. Agric. Food Chem.* **2020**, *68*, 12702−12709.
(26) Biesuz, R.; Quadrelli, P.; Magnaghi, L. R. Sensori per la Valutazione della Qualità di Prodotti Alimentari a Base di Carne. U.S. Patent 10201900000464, 2019.
(27) Biesuz, R.; Quadrelli, P.; Magnaghi, L. R. Sensors for the Evaluation of the Quality of Meat-Based Food. WIPO PCT IB2020/052998, 2020.
(28) Casula, R.; Crisponi, G.; Cristiani, F.; Nurchi, V. M.; Casu, M.; Lai, A. Characterization of the ionisation and spectral properties of sulfonephtalein indicators. Correlation with substituent effects and structural features. *Talanta* **1993**, *40*, 1781−1788.
(29) Aragoni, M. C.; Arca, M.; Crisponi, G.; Nurchi, V. M.; Silvagni, R. Characterization of the ionisation and spectral properties of sulfonephtalein indicators. Correlation with substituent effects and structural features. Part II. *Talanta* **1995**, *42*, 1157−1163.
(30) Sabnis, R. W. *Handbook of Acid-Base Indicators*; Taylor and Francis Group: Oxfordshire, U.K., 2008.
(31) Ruiz, C.; Sànchez-Chaves, M.; Cerrada, M. L.; Fernàndez-Garcìa, M. Glycopolymers Resulting from Ethylene-Vinyl Alcohol Copolymers: Synthetic Approach, Characterisation, and Interactions with Lectins. *J. Polym. Sci., Part A: Polym. Chem.* **2008**, *46*, 7238−7248.
(32) Sànchez-Chaves, M.; Ruiz, C.; Cerrada, M. L.; Fernàndez-Garcìa, M. Novel glycopolymers containing aminosaccharide pendant groups by chemical modification of ethylene-vinyl alcohol copolymers. *Polymer* **2008**, *49*, 2801−2807.
(33) *GNU Image Manipulation Program (GIMP)*. https://www.gimp.org/.
(34) *Chemometric Agile Tool (CAT)*. http://www.gruppochemiometria.it/index.php/software/19-download-the-r-based-chemometric-software.
(35) Sagratini, G.; Fernàndez-Franzòn, M.; De Berardinis, F.; Font, G.; Vittori, S.; Manes, J. Simultaneous determination of eight underivatised biogenic amines in fish by solid phase extraction and liquid chromatography-tandem mass spectrometry. *Food Chem.* **2012**, *132*, 537−543.
(36) Sirocchi, V.; Caprioli, G.; Ricciutelli, M.; Vittori, S.; Sagratini, G. Simultaneous determination of ten underivatized biogenic amines in meat by liquid chromatography-tandem mass spectrometry (HPLC-MS/MS). *J. Mass Spectrom.* **2014**, *49*, 819−825.
(37) Mohr, G. J.; Wolfbeis, O. S. Optical sensors for a wide pH range based on azo dyes immobilized on a novel support. *Anal. Chim. Acta* **1994**, *292*, 41−48.
(38) Mohr, G. J.; Werner, T.; Wolfbeis, O. S.; Janoschek, R. Synthesis of reactive vinylsulphonyl azo dyes for application in optical pH sensing. *Dyes Pigm.* **1994**, *24*, 223−240.
(39) Mohr, G. J.; Müller, H.; Bussemer, B.; Stark, A.; Carofiglio, T.; Trupp, S.; Heuermann, R.; Henkel, T.; Escudero, D.; Gonzàlez, L. Design of acidochromic dyes for facile preparation of pH sensor layers. *Anal. Bioanal. Chem.* **2008**, *392*, 1411−1418.
(40) Seiler, K.; Simon, W. Theoretical aspects of bulk optode membranes. *Anal. Chim. Acta* **1992**, *266*, 73−87.

https://dx.doi.org/10.1021/acsfoodscitech.0c00089
ACS Food Sci. Technol. 2021, 1, 165−175